Journal of Statistical Physics, Vol. 77, Nos. 3/4, 1994

Random Walks with Short-Range Interaction and Mean-Field Behavior

Sergio Caracciolo,[1] Giorgio Parisi,[2] and Andrea Pelissetto[3]

Received December 15, 1993; final May 13, 1994

We introduce a model of self-repelling random walks where the short-range interaction between two elements of the chain decreases as a power of the difference in proper time. The model interpolates between the lattice Edwards model and the ordinary random walk. We show by means of Monte Carlo simulations in two dimensions that the exponent ν_{MF} obtained through a mean-field approximation correctly describes the numerical data and is probably exact as long as it is smaller than the corresponding exponent for self-avoiding walks. We also compute the exponent γ and present a numerical study of the scaling functions.

KEY WORDS: Random Walks; polymer; Monte Carlo; mean field; critical exponent; Flory theory.

1. INTRODUCTION

Self-avoiding walks on a lattice are a fascinating subject. Although they are much simpler than an Ising or Heisenberg spin system, they behave quite similarly in the critical region where the coherence length is much larger than the lattice spacing. There are deep reasons for this similarity. Indeed, using Symanzik representation,[1,2] one can write the free energy of a spin system as sum over partition functions of self-avoiding walks. Moreover, the self-avoiding walks are exactly the limit of an $O(n)$-invariant spin system for n going to zero.[3-6]

[1] Dipartimento di Fisica and INFN, Sezione di Lecce, Università di Lecce, Lecce 73100, Italy. Internet: CARACCIO@UX1 SNS.SNS.IT.

[2] Dipartimento di Fisica and INFN, Sezione di Roma, Università di Roma I "La Sapienza", Rome 00185, Italy.

[3] Dipartimento di Fisica and INFN, Sezione di Pisa, Università degli Studi di Pisa, Pisa 56100, Italy. Internet: PELISSET@SUNTHPI1.DIFI.UNIPI.IT. Bitnet: PELISSET@IPISNSVA.BITNET. Hepnet/Decnet: 39198::PELISSETTO.

0022-4715/94/1100-0519$07.00/0

A long time ago Flory,[7] using simple-minded approximations, found that the critical exponent ν in dimension D less than or equal to 4 was given by the simple expression

$$\nu = 3/(2+D) \tag{1}$$

This result is quite puzzling; it is exact for $D = 1, 2$, and 4, and it is a very good approximation in $D = 3$,[8-11] although in $4-\varepsilon$ dimensions the exact results and Flory's differ at first order in ε.[3] The Flory approximation was strongly criticized by des Cloiseaux,[12,13] but he found the puzzling result that a more accurate variational approximation leads in three dimensions to the rather bad value of $\nu = 2/3$.

Quite recently it was found that des Cloiseaux' method can be extended to the case of polymers with long-range repulsion.[14] Also in this case Flory's and des Cloiseaux' approaches give different results; however, here it is possible to give very strong arguments suggesting that the variational approach of des Cloiseaux gives the exact result in the case where the space dimension becomes infinite.

The putative exact infinite-dimensional results can be extrapolated at finite dimensions using arguments based on the renormalization group and performing the approximation directly at finite dimension. One finally finds that for an interaction which decreases with the distance as a power law with exponent λ, ν is given by the generalization of des Cloiseaux' formula[14]

$$\nu = \begin{cases} 1 & \text{for} \quad \lambda \leqslant 2 \\ 2/\lambda & \text{for} \quad 2 \leqslant \lambda \leqslant 4 \\ 1/2 & \text{for} \quad \lambda \geqslant 4 \end{cases} \tag{2}$$

with logarithmic corrections when $\lambda = 2, 4$.

Some of these predictions have been numerically tested.[15]

The fact that mean-field methods give in the previous case the exact value of ν is not a big surprise, as they usually work well with long-range interactions.[16] It remains unclear, however, if the same approximation can be applied with success to theories with short-range interactions. In this paper we discuss a model for polymers with a potential which is strictly short-range in space, parametrized by an exponent λ which interpolates between the Edwards model[17] ($\lambda = 0$) and the ordinary random walk ($\lambda = \infty$). The mean-field analysis of des Cloiseaux can be trivially extended to this case and a prediction for $\nu_{MF}(\lambda)$ can be derived. In two dimensions we have studied this model with a Monte Carlo simulation and we have found that the observed value of ν is in good agreement with $\max(\nu_{MF}(\lambda), \nu_{SAW})$ with $\nu_{SAW} = 3/4$. Thus this model provides an example of a system

where the interactions are strictly local and where the variational approach gives the exact answer for ν at least for a certain range of the parameters.

The well-confirmed mean-field predictions for the exponent ν do not imply, however, that the critical behavior of the model is really mean-field. In order to clarify this point, we have also studied the critical exponent γ and checked that in mean-field approximation its value is systematically overestimated.

We present the model in Section 2, and in Section 3 we report the computation of ν using the method of des Cloiseaux. The algorithms we use for the numerical simulations are described in Section 4; the results we obtain are presented in Section 5. Some conclusions and a discussion of the results appear in Section 6.

2. THE MODEL

Let $\mathscr{C}$ be the ensemble of random walks on the hypercubic lattice $\mathbf{Z}^D$ of N steps, starting from the origin. Thus, if $\omega \in \mathscr{C}$,

$$\omega = \{\boldsymbol{\omega}_0, \boldsymbol{\omega}_1, \boldsymbol{\omega}_2, ..., \boldsymbol{\omega}_N\} \tag{3}$$

with $\boldsymbol{\omega}_0 = \mathbf{0}$ the origin of the lattice, $\boldsymbol{\omega}_i \in \mathbf{Z}^D$ the location at time i of the walk, and $|\boldsymbol{\omega}_i - \boldsymbol{\omega}_{i-1}| = 1$ for $i = 1, ..., N$.

We consider an interaction of the form

$$H_1[\omega] = \frac{1}{2} g_0 \sum_{\substack{i,j=0 \\ i \neq j}}^{N} \frac{\delta_{\boldsymbol{\omega}_i, \boldsymbol{\omega}_j}}{|i-j|^{\lambda}} \tag{4}$$

This means that in the ensemble average $\langle \cdot \rangle$ in $\mathscr{C}$ we associate to each walk the statistical weight

$$m[\omega] = \frac{e^{-H_1[\omega]}}{Z_N} \tag{5}$$

where

$$Z_N = \sum_{\omega \in \mathscr{C}} e^{-H_1[\omega]} \tag{6}$$

A similar model had been previously considered by Oono.[18]

To study the conformation of the walks in this ensemble, we shall consider the square end-to-end distance

$$R_e^2[\omega] \equiv \boldsymbol{\omega}_N^2 \tag{7}$$

and the square radius of gyration

$$R_g^2[\omega] \equiv \frac{1}{N+1} \sum_{i=0}^{N} \left(\omega_i - \frac{1}{N+1} \sum_{j=0}^{N} \omega_j \right)^2 \tag{8}$$

Both of them are believed to have the asymptotic behavior

$$\langle R^2 \rangle \sim N^{2\nu} \tag{9}$$

as $N \to \infty$, with the same critical exponent ν.

We shall also consider the universal ratio

$$A \equiv \frac{\langle R_g^2 \rangle}{\langle R_e^2 \rangle} \tag{10}$$

For ORW (ordinary random walks) we have $\nu = 1/2$ and $A = 1/6 \sim 0.16667$, while for SAW (self-avoiding walks) ν and A depend on the dimension of the embedding space. In two dimensions we have $\nu = 3/4$,[19] while the most precise estimate for A is obtained by a Monte Carlo simulation[20] whose result is $A = 0.14026 \pm 0.00011$, where the error bar is 95% level of confidence.

We will also compute the exponent γ assumping that for large N

$$Z_N = \mu^N N^{\gamma - 1} \tag{11}$$

where μ is a nonuniversal constant and γ a universal exponent depending only on λ and on the dimensionality of the space D.

For ORW, $\gamma = 1$, while for SAW, γ depends on the dimension D. In two dimensions $\gamma = 43/32 = 1.34375$.[19]

3. MEAN-FIELD ANALYSIS

In this section we want to derive an estimate of the critical exponent ν with a variational approach. Following des Cloiseaux,[12] we consider random rings instead of random walks, as this fact does not change the value of ν and simplifies the calculations by permitting Fourier analysis along the chain. In addition, it is simpler to work in continuum space rather than on a lattice. In this case one must somehow regularize the δ-function appearing in (4). We will thus consider as equilibrium probability measure for the model

$$dm(\omega) = \frac{1}{Z} \exp(-H)\, d^D\omega_1 d^D\omega_2 \cdots d^D\omega_N \tag{12}$$

where the Hamiltonian is given by

$$H=\frac{1}{2}\sum_{i=0}^{N}(\boldsymbol{\omega}_i-\boldsymbol{\omega}_{i-1})^2+\frac{1}{4}g_0\sum_{\substack{i,j\neq 0\\ i\neq j}}^{N}\left(\frac{V[(\boldsymbol{\omega}_i-\boldsymbol{\omega}_j)^2]}{|i-j|^{\lambda}}+\frac{V[(\boldsymbol{\omega}_i-\boldsymbol{\omega}_j)^2]}{(N-|i-j|)^{\lambda}}\right) \tag{13}$$

The second term in the potential has been added in order to guarantee invariance under translations along the chain. Here $V(x^2)$ can be any arbitrary short-range potential and for definiteness we will assume

$$V(x^2)=\exp\left(-\frac{x^2}{2a}\right) \tag{14}$$

The mean-field approximation is based on a variational approach with a Gaussian trial measure[12,14]

$$dm_0(\omega)=\frac{1}{Z_0}\exp(-H_0)\,d^D\boldsymbol{\omega}_1 d^D\boldsymbol{\omega}_2\cdots d^D\boldsymbol{\omega}_N \tag{15}$$

with

$$H_0=\frac{1}{2}\sum_{i,j=0}^{N}G_{ij}^{-1}\boldsymbol{\omega}_i\cdot\boldsymbol{\omega}_j \tag{16}$$

and

$$Z_0=(2\pi)^{(N+1)D/2}(\det G)^{D/2} \tag{17}$$

The function G_{ij} is determined by minimizing the functional

$$F[G]=\langle H-H_0\rangle_0-\log Z_0 \tag{18}$$

where $\langle\cdot\rangle_0$ denotes the expectation value with respect to dm_0.

Because of invariance under translations along the chain we have $G_{ij}=G(i-j)$ and by symmetry $G(n)=G(-n)$. It is also convenient to introduce the Fourier transform

$$\tilde{G}(p)=\sum_{\tau=0}^{N-1}G(\tau)\,e^{ip\tau} \tag{19}$$

where $p=0,\ 2\pi/N,\ \ldots,\ 2\pi(N-1)/N$, and $\tilde{G}(p)$ is real and positive due to the positive-definiteness of G_{ij}.

The functional F can be computed as

$$\frac{F[G]}{N} = D\int_{-\pi}^{\pi}\frac{dp}{2\pi}\tilde{G}(p)(1-\cos p) - \frac{D}{2}[1+\log(2\pi)] - \frac{D}{2}\int_{-\pi}^{\pi}\frac{dp}{2\pi}\log\tilde{G}(p) + \frac{g_0}{2}\sum_{\tau=1}^{\infty}\frac{1}{\tau^{\lambda}}\left[1+\frac{2}{a}\int_{-\pi}^{\pi}\frac{dp}{2\pi}\tilde{G}(p)(1-\cos p\tau)\right]^{-D/2} \tag{20}$$

where we have replaced sums over p with the corresponding integrals, as we are interested in the regime of very large N.

The minimization condition becomes

$$\frac{1}{\tilde{G}(p)} = 2(1-\cos p) - \frac{g_0}{a}\sum_{\tau=1}^{\infty}\frac{1}{\tau^{\lambda}}(1-\cos p\tau) \times\left[1+\frac{2}{a}\int_{-\pi}^{\pi}\frac{dp'}{2\pi}\tilde{G}(p')(1-\cos p'\tau)\right]^{-(D+2)/2} \tag{21}$$

The exponent ν can be extracted, as easily seen, from the low-momentum behavior of $\tilde{G}(p)$ as

$$\tilde{G}(p) \sim \frac{1}{|p|^{2\nu+1}} \tag{22}$$

The analysis of (21) is quite subtle and can be done following the original paper by des Cloiseaux[12] and predicts $\nu = 1/2$ for $D > 4$, while for $D \leqslant 4$ it gives the following result:

$$\nu_{\mathrm{MF}}(\lambda, D) = \begin{cases} \frac{1}{2} & \text{for} \quad \lambda > \frac{1}{2}(4-D) \\ (2-\lambda)/D & \text{for} \quad \max(0, 2-D) < \lambda < \frac{1}{2}(4-D) \end{cases} \tag{23}$$

For $\lambda = 0$, $D = 2$, additional logarithmic corrections appear as

$$\langle R_g^2 \rangle \sim N^2/\log N \tag{24}$$

and analogous for $\lambda = \frac{1}{2}(4-D)$ we get

$$\langle R_g^2 \rangle \sim N(\log N)^{2/D} \tag{25}$$

Thus we obtain an ORW for λ large enough. This has indeed to be expected, as we have the trivial rigorous bound

$$H_1(\omega) < CN^{2-\lambda} \tag{26}$$

showing that at least for $\lambda > 2$ the model is an ORW.

On the other hand, the mean-field result ν_{MF} is definitely wrong for $\lambda = 0$, $D \leqslant 4$, which corresponds to the SAW limit.[12,17] In two and three dimensions ν_{SAW} is equal respectively to 3/4 and approximately 3/5 [see (1)] while $\nu_{MF}(0, D)$ corresponds to 1 and 2/3. For $D = 4$ the mean-field approach correctly predicts logarithmic corrections to the random-walk behavior, but the power of the logarithm is higher than that obtained using the renormalization group, which predicts[21]

$$\langle R_g^2 \rangle \sim N(\log N)^{1/4} \tag{27}$$

Of course the variational approach will overestimate ν also for small λ. We do not have any theoretical control of this regime. However, as we will discuss in Section 5, our numerical results are in reasonable agreement with the following conjecture for $\nu(\lambda, D)$:

$$\nu(\lambda, D) = \min(\nu_{SAW}, \nu_{MF}(\lambda, D)) \tag{28}$$

Let us finally notice that for large N, the mean-field equation (21) has a general scaling solution. Indeed, in the limit of small p, which corresponds to large N, we can rewrite (21) as

$$\frac{1}{p^2 \tilde{G}(p)} = 1 - g_0 \frac{1}{a} \int_0^\infty d\tau\, \tau^{-\lambda} \frac{1 - \cos p\tau}{p^2} \times \left[\frac{2}{a} \int_{-\pi}^{\pi} \frac{dp'}{2\pi} \tilde{G}(p')(1 - \cos p'\tau) \right]^{-(D+2)/2}$$

It is easy to check that the general solution has the form

$$\tilde{G}(p) = \frac{1}{p^2} \hat{f}_\lambda(g_0 p^{\lambda - 2 + D/2}) \tag{30}$$

which gives

$$\langle R_g^2 \rangle = N \hat{f}_\lambda(g_0 N^{2 - \lambda - D/2}) \tag{31}$$

In the previous discussion we have considered the limit $N \to \infty$ with g_0 fixed. Different critical behaviors can be obtained if we let g_0 go to zero or infinity when N goes to infinity. Let us thus study the limit $N \to \infty$ with $g = g_0 N^{-\delta}$ fixed. For simplicity we shall set from now on $D = 2$, the generalization to arbitrary D being trivial.

Let us first consider the case in which $\delta < 0$, namely the case in which we are weakening the coupling constant when approaching the asymptotic limit. One can think of the model in the intermediate region in a perturbative expansion around the ORW, that is, around $g_0 = 0$. To evaluate the

dimension of the coupling constant, remark that $N^{2-\nu D}$ is the asymptotic behavior for large N of the average number of intersections of two walks of N steps and Hausdorff dimension $1/\nu$ on a lattice of dimension D. Then

$$[g] = -[N](\delta - \lambda + 2 - \nu_{\mathrm{ORW}} D) = 2 + 2\delta - 2\lambda \tag{32}$$

and

$$[N] = -\frac{1}{\nu_{\mathrm{ORW}}} = -2 \tag{33}$$

Thus in the scaling region we expect that for gN^{δ} small

$$\langle R_g^2 \rangle = NF_\lambda(g, N) = Nf_\lambda(gN^{1+\delta-\lambda}) \tag{34}$$

Let us notice that for $\delta = 0$ this expression coincides with the scaling formula (31). For $g = 0$ the model is an ORW and thus we get $f_\lambda(0) \neq 0$. It follows that, when $\delta < \lambda - 1$, $\langle R_g^2 \rangle$ scales as N. On the other hand, when $\lambda - 1 \leqslant \delta < 0$ the argument of the scaling function f_λ goes to infinity. Assuming in this limit $f_\lambda(x) \sim x^{\beta}$, with β independent of δ, we get

$$\langle R_g^2 \rangle \sim N^{1+\beta(1+\delta-\lambda)} \tag{35}$$

The value of β is computed using the conjectured value for ν when $\delta = 0$. In this way we obtain that $f_\lambda(x)$ scales for large x as

$$f_\lambda(x) \sim \begin{cases} x^{(2\nu_{\mathrm{SAW}}-1)/(1-\lambda)} \sim x^{1/(2-2\lambda)} & \text{when} \quad 0 \leqslant \lambda \leqslant 1/2 \\ x^{[2\nu(\lambda)-1]/(1-\lambda)} \sim x & \text{when} \quad 1/2 \leqslant \lambda \leqslant 1 \end{cases} \tag{36}$$

Then we obtain the prediction

$$\langle R_g^2 \rangle = \begin{cases} N^{3/2+\delta/(2-2\lambda)} & \text{when} \quad 0 \leqslant \lambda \leqslant 1/2, \quad \delta \geqslant \lambda - 1 \\ N^{2+\delta-\lambda} & \text{when} \quad 1/2 \leqslant \lambda \leqslant 1, \quad \delta \geqslant \lambda - 1 \\ N & \text{when} \quad \lambda \geqslant 1 \text{ and } \lambda < 1, \quad \delta < \lambda - 1 \end{cases} \tag{37}$$

In the opposite situation ($\delta > 0$) the coupling constant goes to infinity while approaching the asymptotic limit and we can expect that in this case the scaling behavior is controlled by the SAW fixed point. Then

$$[N] = -\frac{1}{\nu_{\mathrm{SAW}}} = -\frac{4}{3} \tag{38}$$

and

$$[g] = -[N](\delta - \lambda + 2 - \nu_{\mathrm{SAW}} D) \tag{39}$$

so that we expect that for gN^{δ} large

$$\langle R_g^2 \rangle = N^{2\nu_{SAW}} \bar{F}_{\lambda}(g, N) = N^{3/2} \bar{f}_{\lambda}(gN^{1/2+\delta-\lambda}) \tag{40}$$

Since for g going to infinity at fixed N we expect the model to describe a SAW, $\bar{f}_{\lambda}(x)$ must converge to a constant for large x. It immediately follows that for $\delta > \lambda - 1/2$ the behavior is that of a SAW. On the other hand, when $\delta < \lambda - 1/2$ and $\lambda > 1/2$, the argument of the scaling function goes to zero when N goes to infinity. Since for $g = 0$ we have an ORW, we must have $\bar{f}_{\lambda}(0) = 0$. Then, assuming for small x the scaling form $\bar{f}_{\lambda}(x) \sim x^{\beta}$, we get

$$\langle R_g^2 \rangle \sim N^{3/2+\beta(1/2+\delta-\lambda)} \tag{41}$$

This exponent β is computed by requiring that for $\delta = 0$ this formula reproduces the result (28). We thus get that the scaling function $\bar{f}_{\lambda}$ must scale for small argument as

$$\bar{f}_{\lambda}(x) \sim \begin{cases} x^{[4(\nu(\lambda)-\nu_{SAW})]/(1-2\lambda)} \sim x & \text{when} \quad 1/2 \leqslant \lambda \leqslant 1 \\ x^{4(\nu_{ORW}-\nu_{SAW})/(1-2\lambda)} \sim x^{1/(2\lambda-1)} & \text{when} \quad \lambda \geqslant 1 \end{cases} \tag{42}$$

Then for positive δ we get

$$\langle R_g^2 \rangle = \begin{cases} N^{3/2} & \text{when} \quad 0 \leqslant \lambda \leqslant 1/2 \text{ and } \lambda > 1/2, \quad \delta > \lambda - 1/2 \\ N^{2+\delta-\lambda} & \text{when} \quad 1/2 \leqslant \lambda \leqslant 1, \quad \delta \leqslant \lambda - 1/2 \\ N^{1+\delta/(2\lambda-1)} & \text{when} \quad \lambda \geqslant 1, \quad \delta \leqslant \lambda - 1/2 \end{cases} \tag{43}$$

Let us notice that all these scaling arguments do not take into account logarithmic corrections, which we expect to be present for those values of δ where there is the transition to the purely SAW or ORW behavior.

The exponent ν could also be studied *à la* Flory. In this case the free energy is approximated as a sum of two terms, the former due to the potential energy and the latter to the entropy. Thus

$$F = a \frac{N^{2-\lambda}}{R^D} + b \frac{R^2}{N} \tag{44}$$

which gives by minimization that

$$R^{D+2} \sim N^{3-\lambda} \tag{45}$$

and therefore

$$\nu_F(\lambda) = \frac{3-\lambda}{D+2} \tag{46}$$

valid as long as $\nu_F \geqslant 1/2$. Of course, for $\lambda = 0$ it coincides with the usual Flory result. Moreover, the value of λ such that $\nu_F(\lambda) = 1/2$ coincides with the one such that $\nu_{MF}(\lambda) = 1/2$. This has to be expected: indeed the two main problems of the Flory procedure are the use of the entropy as computed for ORW and the neglecting of correlations among monomers. But both approximations are reasonable for the model where $\nu = 1/2$. In the intermediate region, however, as we shall see in the next section, the Monte Carlo data clearly disagree with the prediction $\nu_F(\lambda)$.

4. THE ALGORITHM

In order to determine ν, we have generated random walks with fixed N distributed according to (4) by using the so-called *pivot* algorithm,[22-24] which is known to be extremely efficient for the simulation of SAWs with fixed number of steps and free endpoints, as the computer time necessary to produce an independent walk is of the order of the number of steps in the walk, which is also the best possible behavior because this is the order of time necessary simply to write down all the steps.

The algorithm is defined as follows.[24] Choose at random a point along the walk (the *pivot*), but not the first or the last one. Let it be the kth point ω_k, with $0 < k < N$. Then choose at random an element g in the symmetry group of the lattice and propose a new walk ω' defined by

$$\omega_i' = \begin{cases} \omega_i & \text{for} \quad 0 \leqslant i \leqslant k \\ \omega_k + g(\omega_i - \omega_k) & \text{for} \quad k+1 \leqslant i \leqslant N \end{cases} \tag{47}$$

The new walk is accepted according to a Metropolis test in order to generate the desired statistical ensemble.

For the limiting case of ORW and SAW it is known[24] that for a global observable A the integrated autocorrelation time $\tau_{\text{int},A}$ scales for large number of steps according to

$$\tau_{\text{int},A} \sim N^p \tag{48}$$

where (the exponent p should be the same for all global variables)

$$p = \begin{cases} 0 & \text{for} \quad \text{ORW} \\ 0.194 \pm 0.002 & \text{for} \quad \text{SAW} \end{cases} \tag{49}$$

For our models, as can be seen from Table I, where we report the integrated autocorrelation time for the end-to-end distance, we obtain similar results. When the values of the parameters are such that the walks are in the same universality class of ORW or SAW, the dynamical behavior

Table I. Integrated Autocorrelation Times for the Pivot Runs for the End-to-End Distance for Selected Values of the Parameters λ, δ, and g and of the Number of Steps N of the Walks[a]

λ	0.00	0.00	0.00	0.00	0.25
δ	−1.00	−0.75	−0.50	−0.25	0.00
g	1.00	2.00	3.00	4.00	1.00
$N=100$	6.27(5)	6.22(5)	7.00(6)	8.07(8)	7.48(7)
$N=200$	6.31(8)	6.24(7)	7.76(10)	9.07(13)	8.53(12)
$N=500$	6.54(8)	6.44(7)	7.99(11)	10.77(17)	9.87(15)
$N=1000$	6.53(8)	6.61(8)	8.62(12)	11.63(20)	11.19(18)
$N=2000$	6.51(8)	6.54(8)	8.74(12)	13.24(23)	13.14(23)
$N=4000$	6.40(8)	6.64(9)	9.59(14)	14.71(27)	15.37(29)
p_ν	0.00	0.05	0.09	0.14	0.19
p	0.00(1)	0.01(1)	0.08(1)	0.15(1)	0.20(1)

[a] p_ν is the value obtained through a linear interpolation for the dynamic critical exponent, and p is the estimate based on a fit from our data.

is compatible with (49). In the intermediate cases for which $1/2 \leqslant \nu \leqslant 3/4$ the dynamic critical exponent p ranges correspondingly within the interval [0, 0.19], and we find that it is in reasonable agreement with a linear interpolation of the form

$$p_\nu = 0.39(2\nu - 1) \tag{50}$$

Let us now discuss the computational complexity. In the practical implementation we used a hash-table with linear probing in order to check for the self-intersections of the walk. In the case of SAWs Madras and Sokal[24] showed that it is particularly convenient to insert the points in the hash-table starting from the pivot point and working outward (and of course stopping as soon as an intersection is detected). In this way the mean work per move turns out to be of order N^{1-p}, thus smaller than the work done by inserting the points without a special order which is of order N. We used in our case a similar trick. Indeed, choosing a random number r uniformly distributed in the unit interval, according to the Metropolis prescription, the proposed walk ω' is accepted if

$$H[\omega'] \leqslant S \equiv H[\omega] - \ln r \tag{51}$$

Our implementation works as follows: after the choice of the pivot point and of the transformation g we choose the random number r and compute the quantity S. Then we begin to construct the new walk and we insert the points in the hash-table starting from the pivot point and working outward. Whenever we find an intersection we sum to the energy of the new walk the contribution from that intersection, but we stop if the

accumulated value is already larger than S, because the proposed walk has to be rejected.[4] In the limiting case of very strong repulsion, when the universality class is the same as that of SAW, this implementation works exactly as the original one devised by Madras and Sokal. In the opposite limiting case, the ORW one, practically all proposed walks will be accepted and thus no improvement can be expected. In the general situation we expect (although we did not check) that the computational work scales as $N^{(1-p)}$, where p is the dynamic critical exponent for global observables and thus, in all cases, that the computer time necessary to produce a statistically independent measurement is of order N.

In order to determine the exponent γ, we have used the recently introduced *join-and-cut* algorithm, which simulates the ensemble of two walks with fixed total number N_{tot} of monomers.[25] There is no interaction between the two walks and the Hamiltonian is simply the sum of the Hamiltonians of the two walks. One sweep of the algorithm consists of two steps:

1. Each walk is first updated using the pivot algorithm.
2. A join-and-cut move is performed: the two walks are concatenated and then cut at a random point. The two new walks are then accepted according to a Metropolis test.

This algorithm is extremely efficient for SAWs. If A is a global observable, the integrated autocorrelation time scales for a large number of steps according to

$$\tau_{\text{int},A} \sim N_{\text{tot}}^{p} \tag{52}$$

where

$$p \approx \begin{cases} 0 & \text{for ORW} \\ 0.7 & \text{for SAW} \end{cases} \tag{53}$$

For our models we obtain a similar behavior. When $\lambda \leqslant 1/2$ the dynamical behavior is equal to that of a SAW, while for $1/2 \leqslant \lambda \leqslant 1$ the critical behavior interpolates between that of a SAW and that of an ORW. In Table II we report the autocorrelation time for $\log N_1$, where N_1 is the length of the first walk, from which we get

$$p \approx \begin{cases} 0.45(5) & \text{for } \lambda = 0 \\ 0.49(4) & \text{for } \lambda = 0.25 \\ 0.10(1) & \text{for } \lambda = 0.75 \end{cases} \tag{54}$$

[4] This procedure works because the interaction is repulsive. For attractive interactions, such as for SAWs or trails at the θ-point, the whole new walk must be defined and therefore the mean work per pivot move will scale as the number of steps N. A similar trick was implemented in the study of the Edwards model in ref. 26.

Table II. Integrated Autocorrelation Times for the Join-and-Cut Runs for log N_1[a]

λ	0.00	0.25	0.75
g_0	2.00	1.00	1.00
$N=2000$	13.32(0.48)	8.12(0.23)	1.65(0.02)
$N=4000$	17.88(0.74)	11.66(0.39)	1.71(0.02)
$N=8000$	25.30(1.76)	15.81(0.69)	1.90(0.02)
p	0.45(5)	0.49(4)	0.10(1)

[a] p is the estimated dynamic critical exponent.

Turning now to the practical implementation of the algorithm, we have used the method presented in ref. 25, Section 3.2, and applied the same trick used for the pivot algorithm in order to detect Metropolis failures early. In this way each join-and-cut move is expected to have a cost of order $N_{\text{tot}}^{2-\gamma}$. Thus, as in the original algorithm for the SAW, the computational complexity is dominated by the pivot moves and thus we expect also in this case that the CPU time per iteration scales as N_{tot}^{1-p}.

5. NUMERICAL RESULTS

In order to test the ideas presented in Section 3, we have performed an extensive Monte Carlo simulation on a square lattice on walks of lengths ranging from 100 to 8000.[5] The total CPU time for these runs was roughly 5000 hours of a VAX 6000-520.

We have first of all measured ν using the pivot algorithm. The first problem one has to deal with is the initialization, that is, for each value of λ, δ, g, and N one has to generate a starting walk. This was done in two different ways according to the value of N. When N was less than or equal to 2000 we generated a SAW using a dimerization routine.[27-29,24] When instead $N=4000$, 8000, as the dimerization routine is too costly (the computer time needed to generate a walk scales as $\tau \sim N^{a \log_2 N + b}$, with $a \approx 0.17$ and $b \approx 0.72$ in two dimensions), we used the scanning method[30] with scanning parameter equal to 3.[6] Neither method generates a random sample of walks with the correct equilibrium distribution, although the first

[5] For the Edwards model ($\lambda = 0$) an extensive numerical study is presented in ref. 26.

[6] The only reason we used the dimerization routine for the low-N runs was its availability at the time of the runs. In retrospect it would have probably been more convenient to use the scanning program in all cases.

Table III. Values of $R_\bullet^2$ for $\delta \leqslant 0$[a]

δ	g	100	200	500	1000	2000	4000	8000
$\lambda = 0$								
−1	10.0	207(1)	414(2)	1045(6)	2071(12)	4169(24)	8284(48)	
−3/4	2.0	175(1)	369(2)	1016(5)	2187(12)	4702(26)	10158(58)	
−3/4	5.0	249(1)	541(3)	1504(8)	3268(18)	7084(38)	15342(86)	
−3/4	8.0	307(1)	669(3)	1874(10)	4062(122)	8876(50)	19390(108)	
−1/2	1.0	207(1)	477(3)	1460(8)	3475(19)	8148(46)	19273(108)	
−1/2	3.0	332(1)	786(4)	2480(13)	5871(33)	14000(80)	33389(198)	
−1/2	5.0	417(1)	1000(5)	3164(18)	7624(44)	18227(110)	42895(264)	
−1/4	1.0	341(1)	876(5)	3071(17)	7980(46)	20780(124)	54207(350)	140178(932)
−1/4	2.0	462(2)	1203(7)	4285(25)	11087(68)	28817(188)	75441(518)	
−1/4	4.0	612(2)	1621(9)	5815(36)	15225(100)	39867(274)	104450(754)	
$\lambda = 0.25$								
−3/4	10.0	257(1)	519(3)	1318(8)	2671(15)	5372(31)	10747(64)	
−1/2	5.0	322(1)	716(4)	2088(12)	4689(27)	10379(61)	23336(138)	
−1/2	10.0	458(2)	1052(6)	3092(18)	6964(41)	15736(96)	35485(214)	
−1/2	34.0	726(3)	1859(11)	6034(39)	14344(94)	32933(222)	74819(522)	
−3/8	5.0	430(2)	1035(6)	3251(19)	7746(47)	18399(116)	43618(270)	
−3/8	13.0	658(3)	1667(10)	5513(35)	13613(89)	32933(222)	79261(456)	
−1/4	0.7	212(1)	507(3)	1615(9)	4001(23)	9708(57)	23969(140)	
−1/4	4.7	552(2)	1405(8)	4842(30)	12376(81)	31353(214)	78563(550)	
0	1.0	458(2)	1259(7)	4842(30)	13613(89)	37872(266)	106280(806)	
$\lambda = 0.5$								
−1/2	22.0	529(2)	1176(7)	3174(20)	6640(42)	13593(49)	27748(167)	
−1/4	1.0	193(1)	428(2)	1236(8)	2778(17)	6163(38)	13877(86)	
−1/4	3.3	354(1)	829(5)	2525(16)	5912(37)	13593(49)	31605(204)	72165(472)
−1/4	6.0	488(2)	1168(7)	3690(22)	8784(58)	20578(138)	48194(330)	112036(776)
0	0.5	238(1)	592(3)	2026(12)	5198(32)	13593(49)	35624(232)	
0	1.0	342(1)	888(5)	3174(20)	8390(55)	22322(151)	59257(410)	
0	2.0	502(2)	1339(6)	4925(23)	13215(64)	35925(190)	96580(528)	262693(1550)
0	10.0	767(2)	2133(12)	8320(56)	23177(170)	64877(506)	182090(1524)	506839(4560)
$\lambda = 0.9$								
−1/10	0.2	115.4(0.6)	237.1(1.6)	608(4)	1228(9)	2528(20)	5134(36)	10465(74)
−1/10	0.5	138.4(0.6)	289.7(2.0)	766(5)	1594(11)	3242(22)	6743(46)	13839(96)
−1/10	1.0	174.1(0.8)	373.2(2.5)	1006(7)	2119(14)	4419(30)	9287(65)	19391(135)

[a] All error bars are two standard deviations.

822/77/3-4-2

Table IV. Values of R_e^2 for $\delta > 0$[a]

δ	g	100	200	500	1000	2000	4000	8000
$\lambda = 0.6$								
0	1.0	304(1)	754(5)	2582(16)	6548(42)	16710(113)	42671(303)	
0	2.0	448(2)	1156(7)	4080(27)	10614(74)	27816(205)	71843(552)	
0	4.0	620(3)	1653(10)	6075(42)	16173(118)	43199(344)	113130(980)	
0	5.0	664(3)	1800(11)	6672(48)	17927(136)	48107(390)	129357(1110)	
$\lambda = 0.75$								
0	0.5	182(1)	412(3)	1236(8)	2816(19)	6571(44)	15224(100)	
0	1.0	253(1)	599(4)	1865(12)	4473(30)	10599(72)	24984(174)	
0	5.0	593(3)	1523(10)	5253(39)	13515(106)	33763(288)	84913(750)	
1/10	0.5	224(1)	541(3)	1784(12)	4479(30)	11058(76)	28044(202)	
1/10	1.0	326(1)	829(5)	2845(19)	7275(52)	18615(178)	47802(370)	
1/10	2.0	481(2)	1262(8)	4503(32)	11705(90)	30741(250)	79394(680)	
1/4	1.0	479(2)	1330(9)	5117(38)	14303(112)	40132(342)	111634(1042)	
1/4	2.0	642(2)	1773(12)	6842(50)	19183(148)	53193(450)	147806(1320)	
$\lambda = 0.9$								
0	0.3	136(1)	290(2)	789(5)	1678(11)	3605(25)	7703(54)	16455(114)
0	0.5	160(1)	348(2)	967(7)	2127(15)	4579(32)	10022(68)	21777(145)
0	1.0	214(1)	479(3)	1400(9)	3131(22)	6943(51)	15525(110)	34318(244)
2/10	0.2	159(1)	367(2)	1141(8)	2727(19)	6593(46)	16116(116)	39180(288)
2/10	0.5	240(1)	596(4)	1990(14)	5003(37)	12662(96)	31804(252)	80928(675)
2/10	1.0	353(2)	911(6)	3169(24)	8116(64)	21001(176)	53719(482)	135749(1290)
$\lambda = 1$								
0	0.1	109.2(0.5)	224.0(1.6)	571(4)	1167(8)	2393(17)	4861(34)	9866(70)
0	0.5	148.5(0.7)	318.8(2.2)	857(6)	1810(12)	3824(27)	8104(56)	17021(122)
0	1.0	192.8(0.9)	426.3(2.8)	1190(8)	2569(18)	5541(39)	11879(84)	25536(186)
1/3	0.2	187.7(0.9)	462(3)	1563(11)	4016(30)	10389(80)	26944(220)	70143(616)
1/3	0.5	299.3(1.4)	784(5)	2829(22)	7512(62)	19567(172)	51537(478)	133100(1334)
1/3	1.00	438(2)	1176(8)	4245(34)	11248(96)	29304(277)	77797(771)	203511(2172)
1/3	2.15	600(3)	1621(11)	5906(46)	15923(133)	42261(385)	112434(1100)	
1/2	1.41	686(7)	1907(18)	7389(71)	20805(210)	55614(492)	154556(1444)	435115(4298)
1/2	1.79	729(8)	2038(25)	7901(70)	22182(208)	58609(504)	163330(1532)	459835(4484)
1/2	2.83	706(8)	2000(23)	7897(70)	22483(208)			
2/3	1.00	655(6)	1820(12)	7091(86)	19756(185)			

[a] All error bars are two standard deviations.

is exact in the SAW limit and the second in the ORW one. It was thus necessary to run a certain number of thermalization iterations before measuring. As the convergence to equilibrium of a Markov chain is controlled by the exponential autocorrelation time τ_{exp}, it is necessary to run a few τ_{exp} iterations to reach equilibrium. For the pivot algorithm τ_{exp} is proportional to N. For this reason we ran approximtely $10N$ pivot iterations for thermalization before measuring. For each value of λ, δ, g, and N we then performed 10^6 iterations, except when $N = 100$, in which case the runs consist of 2×10^6 iterations. The integrated autocorrelation times for the squared end-to-end distance and for the square radius of gyration range from 3 to 20 and from 5 to 60, respectively. We have reported a few of them in Table I.

In Table III and IV we report the results of our runs for $\langle R_e^2 \rangle$ for different values of the parameters, respectively for negative and positive values of δ.

We have performed least-squares regressions on these data in order to determine the critical exponent ν. We fit $\langle R_e^2 \rangle$ to the ansatz $aN^{2\nu}$ by performing a weighted least-squares regression of its logarithm against $\log N$, using the *a priori* error bars on the raw data points to determine both the weights and the error bars. In order to control the systematic error due to corrections to scaling, we have done various fits in which the data points with lowest N were discarded. The results of these fits are reported in Table V and VI for various N_{cut}, where N_{cut} is the minimum N included in the fit. In many cases one sees a systematic drift of the estimated exponent with N_{cut}, an indication of strong corrections to the scaling. This effect is, however, strongly dependent on the value of g. When the expected value of ν is different from 1/2 and 3/4 one observes that for for g small the estimated value of ν increases with N_{cut}, while for g large the estimate decreases. For the intermediate values of g there is a flatness region where ν remains approximately constant, meaning that for these values the g-dependent corrections are small compared to our statistical error. For every λ and δ we have made various runs for different values of g in order to find the flat region where the corrections are small enough, in order to obtain estimates of ν with a smaller systematic error. Our final estimates are in reasonable agreement with the proposed value of ν, the discrepancy being less than a few percent. The worst cases are for $\lambda = 1$ and $\lambda = 0.5$. For instance, for $\delta = 1/3$, $\lambda = 1$ our data suggest $\nu \approx 0.68$, 0.69, while the expected value is $\nu = 2/3 \approx 0.667$. Let us notice, however, that for $\lambda = 1$ and $\lambda = 0.5$ we expect the presence of logarithmic corrections, i.e., a behavior of the form

$$\langle R_e^2 \rangle_N = aN^{2\nu} \log^{\beta} N(1 + O(1/\log N, \log\log N/\log N)) \qquad (55)$$

Table V. Values of ν_{eff} for $\delta \leqslant 0$, for Various Values of N_{cut}

δ	g	100	200	500	1000	2000	4000	ν_{th}
$\lambda = 0$								
−1	10.0	0.5003(8)	0.5000(12)	0.4985(19)	0.4999(30)	0.4953(59)		0.5000
−3/4	2.0	0.5505(8)	0.5532(12)	0.5534(18)	0.5538(29)	0.5556(58)		0.5625
−3/4	5.0	0.5588(8)	0.5585(12)	0.5584(18)	0.5578(29)	0.5575(56)		
−3/4	8.0	0.5617(8)	0.5616(12)	0.5621(18)	0.5638(28)	0.5637(57)		
−1/2	1.0	0.6141(8)	0.6178(12)	0.6199(18)	0.6179(28)	0.6210(57)		0.6250
−1/2	3.0	0.6246(8)	0.6255(12)	0.6253(19)	0.6269(30)	0.6270(59)		
−1/2	5.0	0.6290(8)	0.6284(12)	0.6272(19)	0.6232(30)	0.6174(62)		
−1/4	1.0	0.6869(7)	0.6884(10)	0.6895(14)	0.6894(20)	0.6886(32)	0.6854(67)	0.6825
−1/4	2.0	0.6902(9)	0.6901(13)	0.6894(20)	0.6915(33)	0.6942(68)		
−1/4	4.0	0.6969(9)	0.6952(14)	0.6945(22)	0.6946(35)	0.6948(72)		
$\lambda = 0.25$								
−3/4	10.0	0.5068(8)	0.5062(12)	0.5046(19)	0.5022(30)	0.5002(60)		0.5000
−1/2	5.0	0.5807(8)	0.5810(12)	0.5797(19)	0.5787(30)	0.5844(60)		0.5833
−1/2	10.0	0.5897(8)	0.5872(13)	0.5869(19)	0.5873(31)	0.5866(62)		
−1/2	34.0	0.6329(9)	0.6177(14)	0.6051(22)	0.5958(35)	0.5919(70)		
−3/8	5.0	0.6263(8)	0.6246(13)	0.6243(20)	0.6233(31)	0.6226(64)		0.6250
−3/8	13.0	0.6513(9)	0.6453(14)	0.6408(21)	0.6354(35)	0.6335(70)		
−1/4	0.7	0.6400(8)	0.6439(12)	0.6476(19)	0.6457(30)	0.6520(60)		0.6666
−1/4	4.7	0.6732(9)	0.6723(14)	0.6703(21)	0.6667(34)	0.6626(71)		
0	1.0	0.7378(9)	0.7404(14)	0.7423(22)	0.7410(36)	0.7443(75)		0.7500
$\lambda = 0.5$								
−1/2	22.0	0.5382(8)	0.5277(12)	0.5212(20)	0.5158(32)	0.5147(53)		0.5000
−1/4	1.0	0.5794(9)	0.5805(13)	0.5808(20)	0.5801(31)	0.5855(63)		0.6250
−1/4	3.3	0.6076(7)	0.6061(10)	0.6047(15)	0.6026(20)	0.6030(26)	0.5956(66)	
−1/4	6.0	0.6215(7)	0.6187(11)	0.6153(15)	0.6124(22)	0.6112(35)	0.6085(70)	
0	0.5	0.6774(8)	0.6835(12)	0.6893(19)	0.6942(33)	0.6950(54)		0.7500
0	1.0	0.6980(9)	0.7012(14)	0.7039(21)	0.7051(34)	0.7042(70)		
0	2.0	0.7139(6)	0.7153(8)	0.7171(12)	0.7183(17)	0.7174(29)	0.7218(59)	
0	10.0	0.7410(8)	0.7417(12)	0.7415(18)	0.7422(26)	0.7416(43)	0.7384(89)	
$\lambda = 0.9$								
−1/10	0.2	0.5142(8)	0.5135(12)	0.5138(16)	0.5149(23)	0.5124(38)	0.5137(72)	0.5000
−1/10	0.5	0.5258(8)	0.5236(11)	0.5216(16)	0.5206(22)	0.5235(35)	0.5186(70)	
−1/10	1.0	0.5381(8)	0.5352(11)	0.5334(16)	0.5326(22)	0.5334(35)	0.5311(72)	

Table VI. Values of ν_{eff} for $\delta > 0$, for Various Values of N_{cut}

δ	g	100	200	500	1000	2000	4000	ν_{th}
$\lambda = 0.60$								
0	1	0.6698(9)	0.6733(14)	0.6745(22)	0.6761(35)	0.6763(70)		0.7000
0	2	0.6886(9)	0.6898(15)	0.6903(23)	0.6899(37)	0.6845(77)		
0	4	0.7072(10)	0.7063(16)	0.7041(25)	0.7020(41)	0.6945(85)		
0	5	0.7147(10)	0.7134(16)	0.7128(25)	0.7128(41)	0.7135(85)		
$\lambda = 0.75$								
0	0.5	0.5996(9)	0.6023(14)	0.6045(21)	0.6086(34)	0.6061(68)		0.6250
0	1.0	0.6229(9)	0.6234(14)	0.6239(22)	0.6204(35)	0.6186(70)		
0	5.0	0.6745(10)	0.6718(16)	0.6687(26)	0.6628(43)	0.6653(89)		
1/10	0.5	0.6537(9)	0.6582(14)	0.6612(22)	0.6614(35)	0.6713(72)		0.6750
1/10	1.0	0.6754(10)	0.6766(15)	0.6783(24)	0.6790(38)	0.6803(77)		
1/10	2.0	0.6927(10)	0.6918(16)	0.6908(25)	0.6907(41)	0.6844(85)		
1/4	1.0	0.7385(10)	0.7397(17)	0.7416(27)	0.7413(44)	0.7380(91)		0.7500
1/4	2.0	0.7375(10)	0.7386(16)	0.7387(26)	0.7364(42)	0.7372(89)		
$\lambda = 0.90$								
0	0.3	0.5470(8)	0.5476(11)	0.5481(15)	0.5487(22)	0.5476(35)	0.5475(70)	0.5500
0	0.5	0.5608(8)	0.5608(11)	0.5609(16)	0.5598(23)	0.5624(36)	0.5598(71)	
0	1.0	0.5798(8)	0.5788(11)	0.5770(16)	0.5762(23)	0.5763(36)	0.5722(72)	
2/10	0.2	0.6271(8)	0.6336(11)	0.6382(16)	0.6411(23)	0.6428(37)	0.6408(74)	0.6500
2/10	0.5	0.6631(8)	0.6656(12)	0.6679(17)	0.6687(25)	0.6689(41)	0.6737(83)	
2/10	1.0	0.6803(9)	0.6793(13)	0.6787(19)	0.6778(28)	0.6733(46)	0.6687(94)	
$\lambda = 1$								
0	0.1	0.5141(8)	0.5136(12)	0.5139(16)	0.5131(23)	0.5109(36)	0.5106(72)	0.5000
0	0.5	0.5411(8)	0.5394(12)	0.5393(16)	0.5392(23)	0.5386(36)	0.5353(72)	
0	1.0	0.5579(8)	0.5546(11)	0.5529(16)	0.5520(23)	0.5511(37)	0.5521(73)	
1/3	0.20	0.6741(8)	0.6811(13)	0.6859(18)	0.6876(26)	0.6888(42)	0.6902(86)	0.6666
1/3	0.50	0.6972(9)	0.6969(14)	0.6949(20)	0.6921(29)	0.6918(48)	0.6844(99)	
1/3	1.00	0.7014(10)	0.6987(14)	0.6979(21)	0.6969(31)	0.6992(51)	0.6937(105)	
1/3	2.15	0.7099(11)	0.7080(18)	0.7083(28)	0.7049(46)	0.7058(97)		
1/2	1.41	0.7348(13)	0.7341(16)	0.7326(22)	0.7320(32)	0.7418(48)	0.7466(98)	0.7500
1/2	1.79	0.7332(13)	0.7315(17)	0.7302(21)	0.7300(31)	0.7428(47)	0.7467(98)	
1/2	2.83	0.7514(29)	0.7518(46)	0.7547(92)				
2/3	1.00	0.7402(27)	0.7410(35)	0.7391(111)				0.7500

Table VII. Results for the Runs with Higher Statistics and Comparison with the Expected Value for the Exponent ν[a]

	$\lambda = 0.25$		$\lambda = 0.75$	
N	R_e^2	ν	R_e^2	ν
500	4862(10)	0.7433(11)	1874(4)	0.6238(6)
1000	13554(31)	0.7447(17)	4449(10)	0.6239(8)
2000	37927(91)	0.7460(27)	10556(25)	0.6242(13)
4000	106704(277)		25073(60)	
8000	300005(874)		59567(155)	
$\nu(\lambda)$		0.7500		0.6250

[a] In both cases $\delta = 0$ and $g_0 = 1$.

The presence of logarithms makes the analysis very difficult. First of all in this case the convergence to the asymptotic regime is extremely slow. Moreover, the presence of the term $\log^{\beta} N$ makes impossible an evaluation of ν. Indeed, as we use data with $200 \leqslant N \leqslant 8000$, $\log^{\beta} N$ behaves, as far as the fit is concerned, approximately as $N^{\approx 0.3\beta}$. Thus in a pure power-law fit one really measures $2\nu + 0.3\beta$. Since we do not have any theoretical knowledge of β, it is thus impossible to draw any definite conclusion.

To better understand the validity of our conjecture (23), we have made two runs with higher statistics at $\lambda = 0.75$ and $\lambda = 0.25$ with $\delta = 0$.

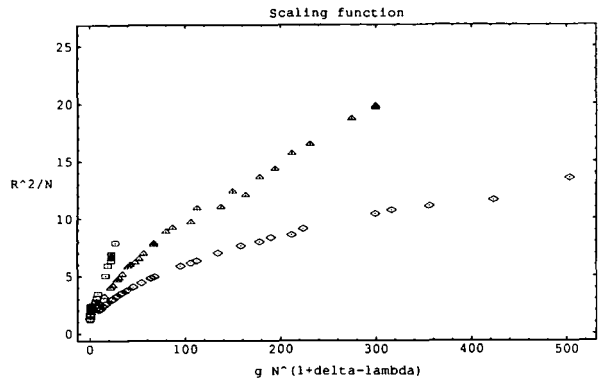

Fig. 1. Scaling function for the end-to-end distance in the case $\delta < 0$. Small pentagons, rectangles, triangles, and diamonds correspond, respectively, to the values $\lambda = 0.90$, 0.50, 0.25, and 0.

Each data point corresponds here to 9×10^6 iterations and in order to avoid any initialization bias we have discarded the first $100\,N$ iterations. The results are reported in Table VII. A good agreement is seen, although a systematic trend is visible in both cases. These results clearly support the claim that our conjectured value for ν is really exact.

We then checked if $\langle R_e^2 \rangle$ obeys the scaling laws (31) and (40). In Fig. 1 we plot our estimates of $\langle R_e^2 \rangle / N$ versus $N^{1+\delta-\lambda}$ for $\delta < 0$ and $\lambda = 0.00,\ 0.25,\ 0.50,\ 0.90$ with $N > 200$. The agreement seems quite good. However, a more detailed examination of the scaling plot shows that the data points do not belong to a unique curve within errors bars. Indeed, one sees that different runs with the same values of g and δ belong to distinct curves which approach each other only when N becomes large. This fact has to be expected. Indeed, as the analysis of the exponent ν shows, for the values of N which we are considering the corrections to scaling are still large and thus we expect analogously large violations to the scaling behavior given by (40). Analogously in Fig. 2 we plot our estimates $\langle R_e^2 \rangle / N^{3/2}$ versus $N^{1/2+\delta-\lambda}$ for $\delta > 0$ and $\lambda = 0.75,\ 0.90$ and $N > 200$. Here again the agreement is only approximate. The situation is even worse for $\lambda = 1.00$ and $\delta > 0$: in this case the points are scattered and no scaling can be observed. This can be explained by the presence of logarithmic terms, which break the scaling laws and make the approach to the asymptotic regime extremely slow. As a final check we studied the behavior of the universal ratio A, which, using the scaling laws (31) and (40), must have the form

$$A = h_\lambda(gN^{1+\delta-\lambda}) \tag{56}$$

for $\delta < 0$ and

$$A = \bar{h}_\lambda(gN^{1/2+\delta-\lambda}) \tag{57}$$

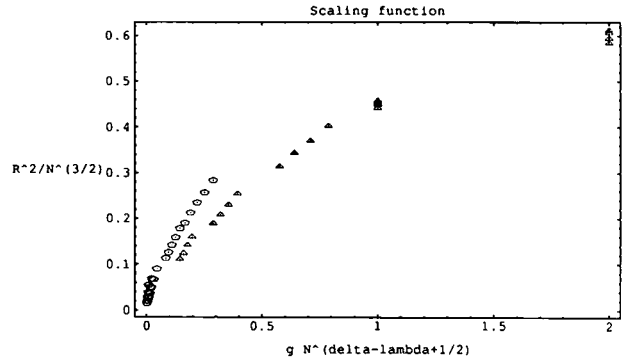

Fig. 2. Scaling function for the end-to-end distance in the case $\delta > 0$. Small pentagons and triangles correspond, respectively, to the values $\lambda = 0.90$ and 0.75.

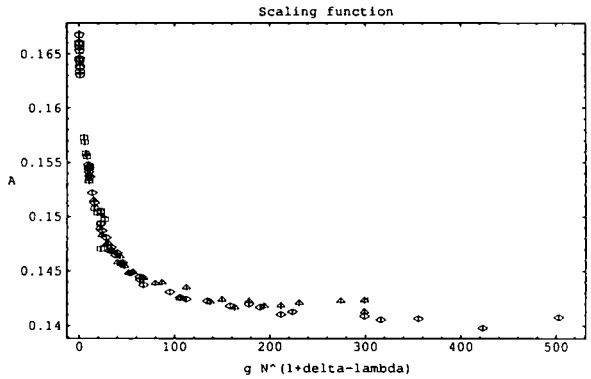

Fig. 3. Scaling function for the universal ratio A in the case $\delta < 0$. Small pentagons, rectangles, triangles, and diamonds correspond, respectively, to the values $\lambda = 0.90$, 0.50, 0.25, and 0.

for $\delta > 0$. Moreover, for $x \to 0$ both functions must converge to the ORW value 1/6. In Figs. 3 and 4 we present the scaling plots for A in the two cases. The agreement is reasonable, although a closer inspection shows again the presence of systematic deviations.

We have also computed the exponent γ. In this case we expect $\gamma = \gamma_{\mathrm{SAW}} = 43/32$ for $\lambda \leqslant 0.5$, where the walk behaves like a SAW, $\gamma = 1$ for $\lambda \geqslant 1$, where we have ORW behavior; however, we do not have any reliable prediction for the intermediate regime $1/2 \leqslant \lambda \leqslant 1$. Indeed the simple variational approach with a Gaussian trial function that we have reported in the previous section always predicts

$$\eta = 0 \tag{58}$$

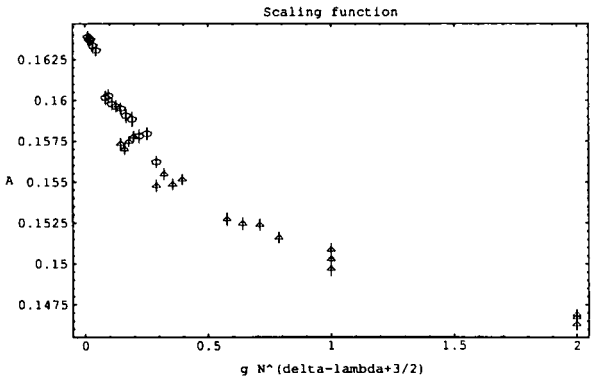

Fig. 4. Scaling function for the universal ratio A in the case $\delta > 0$. Small pentagons and triangles correspond, respectively, to the values $\lambda = 0.90$ and 0.75.

Table VIII. Estimes of γ as a Function of N_{min}

λ	0.00	0.25	0.75
g_0	2.00	1.00	1.00
$N_{min} = 100$	1.339(7)	1.344(3)	1.217(2)
$N_{min} = 200$	1.338(9)	1.344(5)	1.216(2)
$N_{min} = 300$	1.334(12)	1.347(7)	1.216(3)
$N_{min} = 400$	1.330(14)	1.344(8)	1.218(3)
$N_{min} = 500$	1.337(16)	1.346(9)	1.221(3)
$N_{min} = 600$	1.343(19)	1.340(10)	1.224(4)
$N_{min} = 700$	1.342(12)	1.333(11)	1.221(4)

and thus

$$\gamma = (2 - \eta)\nu = 2\nu \tag{59}$$

Therefore, even in the region of λ where the walks behave like SAW, the previous formula gives a wrong prediction ($2\nu = 3/2$). Presumably (59) always overestimates the true γ. We computed γ only for three values of λ, $\lambda = 0.0$, 0.25, 0.75. For each value of λ we made three runs with the join-and-cut algorithm with $N_{tot} = 2000$, 4000, 8000. For the two lowest values of N_{tot} we performed 5×10^7 iterations, while in the last case we did 2.5×10^7 iterations. In each case the starting configuration was a couple of walks of length $N_{tot}/2$ thermalized at the given values of λ and g_0 using the pivot algorithm. The first N_{tot} iterations were subsequently discarded in order to guarantee equilibration. To evaluate γ, we used the maximum-likelihood method as presented in ref. 25, Sections 4 and 5.2. We did not include any correction-to-scaling term, but made fits where the data with N_1, $N_2 < N_{min}$ were systematically discarded. The results are reported in Table VIII. For $\lambda = 0.0$, 0.25 the estimate is clearly compatible with $\gamma_{SAW} = 43/32$, while for $\lambda = 0.75$ we obtain $\gamma(0.75) = 1.221 \pm 0.004 \pm 0.003$, which shows that in the intermediate region also $\gamma(\lambda)$ is a continuous function of λ.

6. CONCLUSIONS

In this paper we have studied a new model for random walks. Its interesting feature is that, although the interacion is strictly local, the mean-field Gaussian approximation gives the correct exponent ν as long as $\nu \leqslant \nu_{SAW}$. This shows that mean-field methods can be applied with success also to short-range models. On the contrary, the Flory approximation,

which is so successful for the SAW, gives a value for ν which disagrees with the numerical data, except for $\lambda = 0$ (Edwards model) and for $\lambda \geqslant 1$ (ORW universality class). It must be noted that although ν is correctly predicted by a mean-field calculation, the model does not really show mean-field behavior. Indeed the exponent γ is not in agreement with the mean-field prediction $\gamma = 2\nu$.

In order to clarify why the Gaussian approximation works so well for $\lambda \geqslant 0.5$ we studied $P(\mathbf{r}, t)$, the probability that $\omega_t - \omega_0 = \mathbf{r}$. For large N, $P(\mathbf{r}, t)$ obeys a scaling law of the form $P(\mathbf{r}, t) = t^{-\nu d} f(r/t^{\nu})$. The variational approximation assumes $f(x)$ to be a Gaussian peaked at $x = 0$, and this is indeed the behavior we found for $\lambda = 0.75$. Thus in this case the variational ansatz is a good approximation to the correct distribution, thereby explaining the agreement between the observed and the mean-field values of ν. On the other hand, for $\lambda = 0.25$, $f(x)$ vanishes for $x = 0$. In this case the variational approximation overestimates the potential energy: indeed, since the interaction is local, the main contribution comes from small values of x and here the variational distribution is much larger than the true one. As a consequence the chain is overswelled and ν is overestimated. Let us notice that, for a SAW in the particular case in which $|\mathbf{r}|$ equals the lattice spacing a, the probability $P(a, t)$ is the relative number of polygons with respect to the total number of walks starting from the origin ω_0. This ratio is expected to behave asymptotically as

$$P(a, t) \sim t^{\alpha - 1 - \gamma} \tag{60}$$

with α satisfying the hyperscaling relation $2 - \alpha = d\nu$. This means that one can estimate the behavior of $f(x)$ for small x, finding $f(x) \sim x^p$ with $p = (\gamma - 1)/\nu = 11/24$. For our model this relation does not hold. This is a reflection of the fact that, except in the well-known limiting case $\lambda = 0$, the model is not described by a quantum field theory.

To conclude, let us notice that in order to obtain more quantitative information beyond the mean-field approximation, one has to resort to the renormalization group approach, which in this case should be implemented directly on the random-walk model, as was done, for example, for the SAW.[13] It would be interesting if a similar study could be done also for the model considered here.[7]

[7] Unfortunately we do not believe that it is enough to renormalize only the non-local coupling as is done in ref. 18, but that also local counterterms should be introduced. The introduction of two couplings is particularly necessary near the point at which the local behavior is recovered. A similar approach in another context can be found in ref. 31. For a renormalization group study of polymers with long-range interaction see also ref. 32. We think that this is the reason the estimate of the exponent ν obtained in ref. 18 does not agree with our result.

Note Added. After the completion of this article we got independent support for our conjectured prediction for the exponent ν. Tom Kennedy[33] gently communicated us that he was able to prove that for $D=1$ the model we consider has $\nu=1$ for $\lambda<1$, that is, when $\nu_{SAW}=\nu_{MF}(\lambda, 1)$, while he finds heuristic arguments based on a renormalization group analysis in real space to get $\nu=1/2$ for $\lambda>3/2$, in full agreement with our formulas.

ACKNOWLEDGMENTS

S. C. and A. P. wish to thank Alan D. Sokal for useful discussions. S. C. is grateful to the Scuola Normale of Superiore of Pisa for kind hospitality.

REFERENCES

1. K. Symanzik, Euclidean quantum field theory, in *Local Quantum Field*, Jost, ed. (Academic Press, New York, 1969); *J. Math. Phys.* 7:510 (1966).
2. D. Brydges, J. Fröhlich, and T. Spencer, *Commun. Math. Phys.* **83**:123 (1982).
3. P. G. de Gennes, *Phys. Lett.* **38A**:339 (1972).
4. J. des Cloiseaux, *J. Phys.* (Paris) **36**:281 (1975).
5. M. Daoud, J. P. Cotton, B. Farnoux, G. Jannink, G. Sarma, H. Benoit, R. Duplessix, C. Picot, and P. G. de Gennes, *Macromolecules* **8**:804 (1975).
6. V. J. Emery, *Phys. Rev. B* **11**:239 (1975).
7. P. J. Flory, *Principles of Polymer Chemistry* (Cornell University Press, Ithaca, New York, 1953).
8. J. C. Le Guillou and J. Zinn-Justin, *Phys. Rev. B* **21**:3976 (1980); *J. Phys.* (Paris) **50**:1365 (1989).
9. A. J. Guttmann, *J. Phys. A* **22**:2807 (1989).
10. E. J. Janse van Rensburg, S. G. Whittington, and N. Madras, *J. Phys. A* **23**:1589 (1990).
11. S. Caracciolo, G. Ferraro, and A. Pelissetto, *J. Phys. A* **24**:3625 (1991).
12. J. des Cloiseaux, *J. Phys.* (Paris) **31**:715 (1970).
13. J. des Cloiseaux and G. Jannink, *Les Polymères en Solution* (Les Editions de Physique, Paris, 1987) [English transl., *Polymers in Solution: Modelling and Structure* (Oxford University Press, Oxford, 1990)].
14. J.-P. Bouchaud, M. Mézard, G. Parisi, and J. S. Yedidia, *J. Phys. A* **24**:L1025 (1991).
15. E. Marinari and G. Parisi, *Europhys. Lett.* **15**:721 (1991).
16. J. Sak, *Phys. Rev. B* **8**:281 (1973); *Phys. Rev. B* **15**:4344 (1977); J. Honkonen and M. Y. Nalimov, *J. Phys. A* **22**:751 (1989).
17. S. F. Edwards, *Proc. R. Soc. Lond.* **85**:613 (1965); C. Domb and G. S. Joyce, *J. Phys. C* **5**:956 (1992).
18. Y. Oono, *Phys. Rev. A* **30**:986 (1984).
19. B. Nienhuis, *Phys. Rev. Lett.* **49**:1062 (1982).
20. S. Caracciolo, A. Pelissetto, and A. D. Sokal, *J. Phys. A* **23**:L969 (1990).
21. A. I. Larkin and D. E. Khmel'nitskii, *Zh. Eksp. Teor. Fiz.* **56**:2087 (1969) [English transl., *Sov. Phys. JETP* **29**:1123 (1969)].
22. M. Lal, *Mol. Phys.* **17**:57 (1969).

23. B. MacDonald, N. Jan, D. L. Hunter, and M. O. Steinitz, *J. Phys. A* **18**:2627 (1985).
24. N. Madras and A. D. Sokal, *J. Stat. Phys.* **50**:109 (1988).
25. S. Caracciolo, A. Pelissetto, and A. D. Sokal, *J. Stat. Phys.* **67**:65 (1992).
26. Ph. de Forcrand, J. Pasche, and D. Petritis, *J. Phys. A* **21**:3771 (1988).
27. K. Suzuki, *Bull. Chem. Soc. Japan* **41**:539 (1968).
28. Z. Alexandrowicz, *J. Chem. Phys.* **51**:561 (1969).
29. Z. Alexandrowicz and Y. Accad, *J. Chem. Phys.* **54**:5338 (1971).
30. H. Meirovitch, *J. Phys. A* **15**:L735 (1982); *J. Chem. Phys.* **79**:502 (1983); *J. Chem. Phys.* **81**:1053 (1984); *Int. J. Mod. Phys. C* **1**:119 (1990).
31. A. Weinrib and B. I. Halpering, *Phys. Rev. B* **27**:419 (1983).
32. P. Pfeuty, R. M. Velasco, and P. G. de Gennes, *J. Phys. Lett.* (Paris) **38**:L5 (1977).
33. T. Kennedy, Ballistic behavior in a 1-d weakly self-avoiding walk with decaying energy penalty, preprint (1994).